Atmos. Chem. Phys. Discuss., 9, 837–863, 2009
www.atmos-chem-phys-discuss.net/9/837/2009/


Atmospheric Chemistry and Physics Discussions

This discussion paper is/has been under review for the journal *Atmospheric Chemistry and Physics (ACP)*. Please refer to the corresponding final paper in *ACP* if available.

# Variability and trends in stratospheric $NO_2$ in Antarctic summer, and implications for the Brewer-Dobson circulation

**P. A. Cook and H. K. Roscoe**

British Antarctic Survey, Madingley Rd, Cambridge CB3 0ET, UK

Received: 1 September 2008 – Accepted: 17 November 2008 – Published: 12 January 2009

Correspondence to: H. K. Roscoe (hkro@bas.ac.uk)

Published by Copernicus Publications on behalf of the European Geosciences Union.





## Abstract

$NO_2$ measurements during 1990–2007, obtained from a zenith-sky spectrometer in the Antarctic, are analysed to determine the long-term changes. The changes in midsummer should be indicative of any changes in the Brewer-Dobson circulation. An atmospheric photochemical box model and a radiative transfer model are used to improve the accuracy of determination of the vertical columns from the slant column measurements, and to deduce the amount of $NO_y$ from $NO_2$. We find that the $NO_2$ and $NO_y$ columns in midsummer have large inter-annual variability superimposed on a broad maximum in 2000, with little overall trend over the full time period. These changes are robust to a variety of alternative settings when determining vertical columns from slant columns or determining $NO_y$ from $NO_2$. They suggest similar changes in speed of the Brewer-Dobson circulation but with opposite sign, i.e. a broad minimum around 2000.

## 1 Introduction

The circulation whereby air enters the stratosphere in the tropics, continues toward the winter pole, and returns to the troposphere via tropopause folds at mid-latitudes, is known as the Brewer-Dobson circulation after its discoverers (Brewer, 1949; Dobson, 1956). It is now known to be driven by the breaking of planetary-scale Rossby waves and of gravity waves, against the mean zonal winds, in the stratosphere and mesosphere. This provides the necessary friction-like force to allow poleward flow on a rotating earth in an otherwise almost frictionless fluid.

Changes in the speed of the Brewer-Dobson circulation will affect the stratospheric concentrations of longer-lived trace gases whose sources are in the troposphere (e.g. CFCs, $CH_4$, $N_2O$), as well as of their eventual stratospheric products (e.g. reactive chlorine gases, $H_2O$, reactive nitrogen gases). Changes in its speed will also affect the tropospheric concentrations of trace gases with large sources in the stratosphere (e.g. ozone). Because these gases are important to atmospheric climate and chemistry, it



ACPD

9, 837–863, 2009



is important to know what changes have occurred to the Brewer-Dobson circulation in the past and will occur in future. A slowing of the circulation would allow more time in the stratosphere for the reactions of $N_2O$ to reactive nitrogen. Hence an upwards trend in the vertical column of reactive nitrogen gases in the stratosphere would indicate a slowing of the circulation.

Tropospheric $N_2O$ is increasing by about 2.5%/decade (WMO 2007), but measured slant columns of $NO_2$ from Lauder, New Zealand (45° S) between 1980 and 1998 show an upwards trend of about 5%/decade (Liley et al., 2000), demonstrating that further processes are involved.

The speed of the Brewer-Dobson circulation will change as planetary and gravity wave intensities are changed, for example due to increased greenhouse gases or to volcanic aerosol. But changes in wave amplitudes are difficult to accurately diagnose from meteorological analyses, particularly for gravity waves, most of which are below the grid scale of current analysis models.

In this paper, we assess trends in stratospheric reactive nitrogen in the hope that it can be used to diagnose changes in the Brewer-Dobson circulation. We examine trends in $NO_2$ in the Antarctic summer, where it is easy to calculate the implied total reactive nitrogen because of the relative absence of $N_2O_5$, an otherwise important component of the reactive nitrogen family. $N_2O_5$ also hydrolyses on aerosol, thereby converting $NO_2$ to $HNO_3$, so its comparative absence in the Antarctic summer means that $NO_2$ is little affected by trends in stratospheric aerosol.

We use $NO_2$ data from a zenith-sky spectrometer that was set up at Faraday in the Antarctic (65.25° S, 64.27° W) between 1990 and 1995, and has now been at the nearby site of Rothera (67.57° S, 68.13° W) since 1996, providing almost continuous measurements of Antarctic $NO_2$ since before the eruption of Mt. Pinatubo (Roscoe et al., 2001; Roscoe, 2004).



ACPD
9, 837–863, 2009



## 2 Apparatus and spectral analysis

Zenith-sky spectrometers, which continuously look at the zenith and record the spectra of scattered sunlight to obtain slant columns of $NO_2$ and ozone, have been used in the Antarctic for many years (Pommereau and Goutail, 1988a, b). The amount of $NO_2$ is analysed by fitting laboratory cross-sections to the observed atmospheric spectrum. Because scattered sunlight is used, the light path through the atmosphere will depend on the Solar Zenith Angle (SZA), and the measurements are of the slant column rather than the vertical column. Because there is no single path of scattered light, the effective slant path length through the atmosphere must be calculated via radiative transfer code. The ratio of this slant path length to the vertical is known as the Air Mass Factor (AMF), equal to about 2 at SZA 60° and about 18 at 90°, but AMF depends on the wavelength of light used and on the vertical profiles of air density and $NO_2$.

The observed spectrum also contains Fraunhofer lines from the atmosphere of the sun, which would interfere with $NO_2$ absorption lines, but because these do not vary with SZA the observed spectra can be divided by a reference spectrum obtained at a small SZA to remove them. This reference spectrum also contains a small slant amount of $NO_2$ which by this division becomes subtracted from the actual slant amounts in the observed spectra.

However there can be significant errors in this method. The spectra are recorded by a solid-state detector with pixels, and because the temperature of the instrument is not controlled it expands and contracts moving the pixels along the spectrum. Due to this wavelength shift each recorded spectrum needs to be interpolated before it can be divided by the reference spectrum. Interpolation causes the narrow Fraunhofer lines to be smoothed and so broadened, hence dividing these broadened lines by the narrower lines in the reference spectrum will create artefacts in the recorded spectra that can interfere with the measurement of the $NO_2$ absorption lines. Hence the amount of $NO_2$ in the reference spectrum will appear to change with the wavelength shift, being a minimum at shifts of 0 or 1 pixels and a maximum at shifts of −0.5 or 0.5. The



ACPD
9, 837–863, 2009



smoothing effect, and so the artefact, is larger if there are fewer pixels within the slit width of the spectrometer.

## 3 Langley plots and their chemical modification

One way of treating the artefact due to wavelength shifts is via Langley plots. On a Langley plot the slant measurements of $NO_2$ are plotted against the associated AMFs to obtain a straight line, the gradient of which gives the vertical column and the intercept gives the negative of the actual amount of $NO_2$ in the reference spectrum plus the artefact (this sum is often called the effective amount in the reference spectrum). To get a useful Langley plot with a large range of AMF at least a half-day of data should be plotted.

Langley plots work well for trace gases which change only slowly during the day such as ozone, but the amount of $NO_2$ varies significantly during the day due to the interchange of $NO_2$ with NO and with reservoir gases such as $N_2O_5$. $NO_2$ reduces quickly at dawn when it is photolysed to NO, then increases quickly at dusk as NO falls almost to zero, while $NO_2$ also increases slowly during the day as $N_2O_5$ is photolysed and reduces slowly during the night as $N_2O_5$ is reformed (e.g. Roscoe et al., 1981).

Hence normal Langley plots cannot be used to accurately determine the vertical column of $NO_2$, instead we must use Langley plots with chemically modified AMFs, AMFs that have been multiplied by the ratio of the $NO_2$ vertical column at that time of day to the $NO_2$ vertical column at sunset (Lee et al., 1994). In the chemically modified Langley plot all of the data points should now lie in a straight line. The intercept from the modified plot is then used with the slant measurements and unmodified AMFs to calculate the $NO_2$ vertical column at twilight (Eq. 1). This method allows Langley plots to be used to improve the accuracy of $NO_2$ vertical columns, and has been used to provide an improved analysis of $NO_2$ measurements between 1990 and 1995 at Faraday (Roscoe et al., 2001).



ACPD
9, 837–863, 2009



## 4 The chemical modification scheme and daily analysis

In order to use this method the variation in $NO_2$ during the course of the day needs to be known for different times of the year. Hence an atmospheric photochemical box model is used to simulate the diurnal variation in $NO_2$ at different times of the year. A radiative transfer model is then used to calculate the AMFs at different SZAs using the profiles of $NO_2$ and ozone calculated by the box model.

We use a variety of models and programs in the scheme, many of which are described by Denis et al. (2005). A photochemical box model is run as 24 stacked boxes to provide the profile through the atmosphere, and includes many different chemical species, gas phase reactions, photochemical reactions and heterogeneous chemical reactions (Chipperfield, 1999), with the amount of aerosol determined by the amount of $H_2SO_4$.

The box model was run for the climatological atmosphere over Faraday and then over Rothera, for 12 individual days in the year at about one month intervals to include both midwinter and midsummer (day numbers 21, 51, 81, 111, 141, 172, 202, 233, 264, 294, 325 and 355), each with a 10 day spin-up at constant day number. The climatology of air pressures, temperatures, and mixing ratios of different chemical species for the start of the runs were provided from the one used by the SLIMCAT atmospheric chemical transport model, interpolated to the required latitude.

The radiative transfer model examines the different paths of scattered sunlight through the atmosphere to the spectrometer, using the profiles of $NO_2$ and ozone from the box model, to calculate the AMFs for $NO_2$ for a range of SZA during the course of each day. Aerosols are not included in this model. For each SZA the model considers multiple light paths through the atmosphere to the zenith sky spectrometer, which are either single scattered or double scattered, and adds up the transmitted light from each path after absorption by a given column of $NO_2$, comparing this to the result with no $NO_2$ column to calculate the AMF (Solomon et al., 1987; Sarkissian et al., 1995).

At large SZA the scattered sunlight follows a long slant path through the atmosphere



ACPD
9, 837–863, 2009



towards the sun, so that the mean SZA for the air mass is less than the SZA directly above the spectrometer. Results from the radiative transfer model show that at SZAs greater than 87° the mean SZA for the air mass only increases at half the rate of the spectrometer SZA, so for spectrometer SZAs of 88° and 89° the air mass SZAs are 87.5° and 88°. So the box model $NO_2$ chemical ratios used by the analysis routine need to be interpolated from the mean air mass SZA rather than the spectrometer SZA.

Finally a program calculates the $NO_2$ vertical column at twilight (87° to 92° SZA), producing both dawn and dusk values for each day where measurements were obtained, by reading large files containing one year of slant measurements, each with the day and time, SZA, detector temperature, wavelength shift, and the measurement error. It uses the $NO_2$ chemical ratios and AMFs from the models to produce modified Langley plots for each day.

Each AMF and chemical ratio ($NO_2$ vertical column relative to the sunset vertical column) used in the Langley plots is calculated by 2-D linear interpolation of the model results according to the SZA and the day number. On each plot a best-fit straight line with error is calculated by weighted least-squares fitting to obtain the intercept and error. A weighted mean of all these intercepts over the whole year of data is calculated. For each slant measurement around twilight an $NO_2$ vertical column is calculated using the mean intercept and the unmodified AMF (Eq. 1), and weighted mean vertical columns are calculated for both dawn and dusk on each day.

$$\text{Vertical\_column} = \frac{\text{Slant\_column} - \text{mean\_intercept}}{\text{AMF}} \quad (1)$$

$NO_2$ vertical columns at dawn and dusk were obtained for almost every day over the period 1990–2007, using in Eq. (1) the weighted mean of the modified Langley plot intercepts between 1 January and 31 December of the relevant year.

The resulting vertical columns at midsummer are examined in more detail by taking the weighted mean of the dawn and dusk columns from days 350–360 (16 to 26 December). One problem when assessing the midsummer trends is that the mean SZA





of the twilight measurements varies, and the $NO_2$ vertical column changes rapidly with SZA at twilight. By using the box model simulation, the measured mean $NO_2$ vertical columns at dawn and dusk can be used to estimate the value at sunset (or 89° in the case of Rothera, where the sun never sets in midsummer), and the ratio of $NO_y/NO_2$ at sunset in the model can be used to estimate the $NO_y$ vertical column.

It is tempting to use in Eq. (1) the individual intercepts to calculate the vertical columns for each day but for many days the error on the intercept is much too large to do this, particularly during winter. An alternative is to use estimates for the intercept calculated from the wavelength shift for each day. In principle this could be more accurate since the wavelength shift varies over the course of the year due to thermal expansion and contraction within the spectrometer, and we expect the intercepts of the modified Langley plots to reflect these variations. Using all the data the intercepts from the modified Langley plots were plotted against the wavelength shifts, the resulting relationship was used to provide daily intercepts from the wavelength shift, and the above calculations of midsummer $NO_2$ and $NO_y$ repeated.

In the calculation of $NO_y$, partitioning of nitrogen species will depend on temperature, the amount of ozone (which affects both the amount of UV light and the gas phase chemistry) and the amount of aerosols, so we examined the sensitivity of $NO_2$ diurnal variations and $NO_y/NO_2$ ratios to these quantities.

Profiles of temperature and ozone were obtained from ECMWF, available from the start of 1994 (temperature) and 2002 (ozone). The box model was run with these profiles for midsummer to provide more accurate $NO_2$ vertical columns, diurnal variations and $NO_y/NO_2$ ratios. The radiative transfer model was also re-run using the $NO_2$ and ozone profiles for each year to provide more accurate AMFs.

$NO_2$ vertical columns at dawn and dusk in midsummer were produced using both the observed profiles for each year and the climatology. Only the summer slant measurements were used in these studies, with midsummer mean intercepts (weighted mean of the modified Langley plot intercepts between 1 December and 15 January) and only AMF values and $NO_2$ chemical ratios from day 355 (21 December).



ACPD
9, 837–863, 2009



## 5 Results

Figure 1 shows examples of the daily variation in $NO_2$ and of the Langley plots produced for the analysis. Multiplying the AMFs by the $NO_2$ chemical ratios from the box model moves both the morning and evening values much closer to a single line, although this line curves down at large values of AMF when using SZAs at the spectrometer. Using the mean SZAs for the air mass makes the line straighter and the errors smaller.

The $NO_2$ vertical columns at twilight produced by the analysis are shown in Fig. 2. The difference between dawn and dusk is greatest during autumn and spring due to the large amounts of $N_2O_5$ at these times, and more variation in the $NO_2$ vertical columns is seen in spring when the site, near the edge of the polar vortex, alternately observes air from inside and outside the vortex. The midsummer and midwinter values vary from year to year, and the lower values of $NO_2$ in December 1991 and all of 1992 are due to the Mt. Pinatubo eruption in June 1991. The eruption greatly increased the amount of aerosols in the stratosphere over the following 18 months, leading to increased hydrolysis of both $BrONO_2$ and $N_2O_5$ to $HNO_3$, which titrates $NO_2$ to $HNO_3$. Note that the AMFs in 1991 and 1992 were not changed in this analysis (the error involved is less than 5%, Slusser et al., 1997).

The Langley plot intercepts are shown in Fig. 3. The intercepts have an annual cycle because the wavelength shift varies over the course of the year due to thermal expansion and contraction within the spectrometer. The modified AMFs produce smaller intercepts, particularly in summer, and are closer to the actual slant amount of $NO_2$ in the reference spectrum ($3.5\times10^{15}$ molec/cm$^2$). The annual cycle is smaller since the artefacts are smaller and more constant with modified AMFs.

The modified Langley plot intercepts are plotted against the wavelength shift in Fig. 4. We expect a repeating pattern with smallest negative values at shifts of 0 and 1 and largest negative values at shifts of −0.5 and 0.5, but here they have been displaced to 0.1 and 0.6. The reason for this displacement is uncertain, but we speculate that it is



ACPD
9, 837–863, 2009



related to the spectral analysis program searching for minimum residuals, always from negative to positive wavelength shift. To find the most probable relationship the plot was folded about 0.1 and 0.6 so that all the intercepts lay in the range 0.1 to 0.6, and a best-fit straight line with error was calculated by least-squares fitting.

We now look in detail at the analysed $NO_2$ vertical columns in midsummer, to consider any trends in $NO_y$. The midsummer values are the most useful for this because the $NO_2$ columns are largest here, and the $N_2O_5$ columns smallest so there is little sensitivity in the $NO_y/NO_2$ ratio to the amount of aerosols. Figure 5 shows the midsummer $NO_2$ vertical columns, using annual weighted mean intercepts of Fig. 3, and daily intercepts estimated from the wavelength shift in Fig. 4. Considerable year-to-year variation is seen and the values from 1991 and 1992 are low following the Mt. Pinatubo eruption. The pattern of trend and variability is almost identical using the two methods of analysis, with all differences smaller than the errors.

To check that these year-to-year variations are not due to differences in the mean SZA of the measurements, thereby causing a different part of the daily variation to be observed, the midsummer columns were interpolated to 89° using the daily variation from the box model. The interpolated columns (not shown) coincide very well, the mean difference is only $-0.01\times10^{15}$ molec/cm$^2$, where the dusk and dawn columns have a mean difference of $0.09\times10^{15}$ molec/cm$^2$. This coincidence gives support to the accuracy of the box model simulations. Much the same pattern of trend and variability to that in Fig. 5 is seen, with a broad maximum near 2000. This pattern could be construed as an upwards trend in the $NO_2$ vertical columns between 1990 and 2000 (excluding 1991 and 1992), and a downwards trend after 2000, in which case the gradients of the best-fit lines are given in Table 1. Using wavelength shift intercepts rather than annual mean intercepts again produces a very similar pattern and any differences in the possible trends (Table 1) are not significant.

Variations in the $NO_2$ vertical column do not necessarily follow variations in $NO_y$ since the partitioning of nitrogen species depends on a number of factors, including temperature, ozone and aerosols. The box model was used to investigate the sensitiv-



ACPD
9, 837–863, 2009



ity of the midsummer $NO_2$ vertical column and $NO_y/NO_2$ ratio to these three factors.

Figure 6a shows the sensitivity of the model $NO_2$ vertical column to temperature. Increasing stratospheric temperature increases $NO_2$ while reducing the diurnal variation. These represent large changes in temperature so the sensitivity to realistic changes is modest.

Figure 6b shows the sensitivity to ozone. Changing the ozone column will change the amount of UV light reaching different levels of the atmosphere and will also affect the gas phase chemistry. Increasing the ozone reduces the $NO_2$ at the same altitude, due to the interaction quantified in Eq. (2) (Roscoe et al., 2001), but has little effect on the overall $NO_2$ column because of the compensating effect of reducing sunlight below, thereby increasing $NO_2$ below.

$$[NO]/[NO_2] = K_{(JNO_2)}\exp(1200/T)/[O_3] \quad (2)$$

Figure 6c shows the sensitivity to aerosols, which is set in the box model by changing $H_2SO_4$. Increasing the aerosols slightly reduces the $NO_2$ column as more $HNO_3$ is produced, but the effect is small in midsummer. Figure 6d shows the sensitivity of the $NO_y/NO_2$ ratio to temperature, and the ratio is seen to fall with increasing temperature. Using the temperature, ozone and aerosols in the climatology the box model gives a $NO_y/NO_2$ ratio of 3.8 at 89° SZA in midsummer.

The partitioning of nitrogen species in the box model at midsummer is most sensitive to temperature with some sensitivity to ozone. Hence to better estimate trends in $NO_2$ and $NO_y$, actual rather than climatological temperature and ozone profiles are needed for each year at midsummer. ECMWF analyses provided temperature and ozone profiles over Faraday and Rothera. The box model was run with these profiles, and the radiative transfer model run with the resulting $NO_2$ and ozone profiles. The box model results for midsummer using the observed and climatological profiles are contrasted in Fig. 7. The $NO_2$ daily variations are very similar, though the vertical column is greater with the observed profiles by 0.8% on average and by 2.2% at twilight (87° to 89°).



ACPD
9, 837–863, 2009



P. A. Cook and
H. K. Roscoe



Figure 8 shows the midsummer dawn and dusk columns interpolated to 89°, using the observed profiles and the climatology. The interpolated columns coincide well, the mean difference is again only $-0.01\times10^{15}$ molec/cm$^2$, and they again have much the same pattern of trend and variability as Fig. 5, with a broad maximum near 2000, and the differences from using the climatology or observed profiles are minimal. Again, the pattern could also be construed as an upwards trend before 2000 followed by a downwards trend since, and the gradients of the best-fit lines are given in Table 2.

Figure 9 shows the midsummer $NO_y$ vertical columns using the observed profiles and the climatology. The $NO_y$ columns are reduced when using the observed profiles, but otherwise the trends and variability are very similar. The gradients of the $NO_y$ best-fit lines are given in Table 2.

Hence using observed profiles of temperature and ozone instead of the climatology makes little difference to the $NO_2$ values and the daily variation from the box model, but makes a significant difference to the $NO_y$ values. However the patterns of trend and variability are almost identical irrespective of the method of analysis and irrespective of $NO_2$ or $NO_y$.

## 6 Interpretation and conclusion

The atmospheric photochemical box model, the radiative transfer model and the analysis routine form a useful method to analyse $NO_2$ slant measurements. By creating chemically modified Langley plots, more accurate vertical columns can be calculated, and by using the daily variation of $NO_2$ and the ratio of $NO_y/NO_2$ in the box model the vertical columns of $NO_y$ can be estimated.

The reduction in the $NO_2$ vertical columns in 1991 and 1992, due to increased hydrolysis of $BrONO_2$ and $N_2O_5$ on the aerosols from the Mt. Pinatubo eruption, are clearly seen (Slusser et al., 1997). These years are excluded from further discussion of trends and variability.

The $NO_2$ vertical columns at midsummer produced by this method have only minimal



ACPD
9, 837–863, 2009



changes when different intercept values are used, either weighted annual means or daily values from the wavelength shift. When interpolated to sunset, the dawn and dusk values coincide, giving confidence in the box model simulations. Once again the year-to-year pattern of trend and variability is almost unchanged. It is also almost unchanged when running the models with the observed profiles of temperature and ozone for each year instead of the climatology. All the analyses of $NO_2$ and $NO_y$ columns at midsummer have a broad maximum near 2000, with significant interannual variability superimposed and little overall trend between 1990 and 2007 (the overall trend in $NO_y$ between 1990 and 2007 is less than 1%/decade, with a standard deviation of almost 4%/decade). The pattern could aternatively be construed as an increasing trend before 2000 and a decreasing trend since, in which case if we accept the premise that a slower Brewer-Dobson circulation allows more time for a source gas to react to its product, this suggests that the Brewer-Dobson circulation slowed to a minimum around 2000 and has since speeded up.

Earlier studies at 45°S have identified an increasing trend in $NO_2$ of about 5 %/decade between 1980 and 1998 (Liley et al., 2000). If our measurements from 1990 to 2000 are taken as part of the same trend, our result is much larger at about 14%/decade. To discuss the implications in terms of Brewer-Dobson circulation, we must first subtract the trend in tropospheric $N_2O$, the source of stratospheric $NO_y$, which is increasing by about 2.5%/decade (WMO 2007), in which case our trends would be over four times those of (Liley et al., 2000).

An alternative viewpoint is that the changes in NOy mostly consist of inter-annual variability, much of it at sub-decadal scales but some with longer periods. From this viewpoint, the two sets of results could be consistent, because of the large $NO_2$ amounts observed in the early 1980s by Liley et al. (2000), plus our large maximum in $NO_2$ and $NO_y$ in 2000. If so, changes in the Brewer-Dobson circulation are dominated by decadal and sub-decadal variability, and there was a minimum in 2000.

Other researchers studying the tropical lower stratosphere have also found implied changes in the Brewer-Dobson circulation and anomalies around 2000 that are cor-

related with atmospheric dynamics. Randel et al. (2006) calculated the mean tropical upwelling from the momentum balance in the atmosphere, finding that this decreased during the 1990s but has increased since 2000, and that both temperature and ozone above the tropical tropopause increased at many longitudes during 1999–2001 which are most probably due to changes in the mean tropical upwelling. Rosenlof and Reid (2008) found that the 1999–2001 warming of the tropical lower stratosphere was very pronounced and that this was strongly correlated with the QBO westerly phase.

Garcia-Herrera et al. (2006) found that the results from general circulation models implied that the El Nino Southern Oscillation (ENSO) signal propagates into the middle atmosphere by means of planetary scale Rossby waves, so that vertical wave propagation is enhanced during El Nino events but reduced during La Nina. Zeng and Pyle (2005) found that stratosphere/troposphere exchange increases during El Nino events, but decreases during La Nina. This suggests that the speed of the Brewer-Dobson circulation may depend on ENSO, with a faster circulation during El Nino years (probably resulting in less $NO_y$) and a slower circulation during La Nina years (probably resulting in more $NO_y$). Liley et al. (2000) found an apparent correlation between the $NO_2$ columns measured at 45° S and ENSO with a time lag of 13 months. Hence the large peak in $NO_y$ in 2000 and the smaller peak in 1997 in this study are consistent with the La Nina events in 1998–2000 and 1996.

Quantitative interpretation of our $NO_2$ and $NO_y$ trends in terms of changes to the Brewer-Dobson circulation will be presented in future work.

*Acknowledgements.* Funding was provided by the EU as part of the GEOMON project (contract number 036677). ECMWF operational analyses data and ERA 40 reanalysis data were obtained from the British Atmospheric Data Centre. We thank the WinDOAS authors Michel van Roozendael and Caroline Fayt of IASB, Belgium, and Martyn P. Chipperfield and Wuhu Feng of the School of Earth and Environment, University of Leeds, UK, for the box model and the climatology.





## References


Brewer, A. W.: Evidence for a world circulation provided by the measurements of helium and water vapour distribution in the stratosphere, Q. J. Roy Meteor. Soc., 75, 351–363, 1949.

Chipperfield, M. P.: Multiannual simulations with a three-dimensional chemical transport model, J. Geophys. Res., 104, D1, 1781–1805, 1999.

Denis, L., Roscoe, H. K., Chipperfield, M. P., Van Roozendael, M., and Goutail, F.: A new software suite for $NO_2$ vertical profile retrieval from ground-based zenith-sky spectrometers, J. Quant. Spectrosc. Ra., 92, 321–333, 2005.

Dobson, G. M. B.: Origin and distribution of polyatomic molecules in the atmosphere, Proc. R. Soc. Lon. Ser.-A, 236, 187–193, 1956.

Garcia-Herrera, R., Calvo, N., Garcia, R. R., and Giorgetta, M. A.: Propagation of ENSO temperature signals into the middle atmosphere: A comparison of two general circulation models and ERA-40 reanalysis data, J. Geophys. Res., 111, D06101, doi:10.1029/2005JD006061, 2006.

Lee, A. M., Roscoe, H. K., Oldham, D. J., Squires, J. A. C., Sarkissian, A., Pommereau, J.-P., and Gardiner, B. G.: Improvements to the accuracy of measurements of $NO_2$ by zenith-sky visible spectrometers, J. Quant. Spectrosc. Ra., 52, 5, 649–657, 1994.

Liley, J. B., Johnston, P. V., McKenzie, R. L., Thomas, A. J., and Boyd, I. S.: Stratospheric $NO_2$ variations from a long time series at Lauder, New Zealand, J. Geophys. Res., 105, D9, 11633–11640, 2000.

Pommereau, J.-P. and Goutail, F.: $O_3$ and $NO_2$ ground-based measurements by visible spectrometry during Arctic winter and spring 1988, Geophys. Res. Lett., 15, 8, 891–894, 1988a.

Pommereau, J.-P. and Goutail, F.: Stratospheric $O_3$ and $NO_2$ observations at the southern polar circle in summer and fall 1988, Geophys. Res. Lett., 15, 8, 895–897, 1988b.

Randel, W. J., Wu, F., Vomel, H., Nedoluha, G. E., and Forster, P.: Deceases in stratospheric water vapor after 2001: Links to changes in the tropical tropopause and the Brewer-Dobson circulation, J. Geophys. Res., 111, D12312, doi:10.1029/2005JD006744, 2006.

Roscoe, H. K., Drummond, J. R., and Jarnot, R. F.: Infrared measurements of stratospheric composition. III, The daytime changes of NO and $NO_2$, Proc. R. Soc. Lon. Ser.-A, 375, 507–528, 1981.

Roscoe, H. K., Charlton, A. J., Fish, D. J., and Hill, J. G. T.: Improvements to the accuracy of measurements of $NO_2$ by zenith-sky visible spectrometers II: errors in zero using a more






complete chemical model, J. Quant. Spectrosc. Ra., 68, 337–349, 2001.
Roscoe, H. K.: A review of stratospheric $H_2O$ and $NO_2$, Adv. Space Res., 34, 1747–1754, 2004.
Rosenlof, K. H. and Reid, G. C.: Trends in the temperature and water vapor content of the tropical lower stratosphere: Sea surface connection, J. Geophys. Res., 113, D06107, doi:10.1029/2007JD009109, 2008.
Sarkissian, A., Roscoe, H. K., and Fish, D. J.: Ozone measurements by zenith-sky spectrometers: an evaluation of errors in air-mass factors calculated by radiative transfer models, J. Quant. Spectrosc. Ra., 54, 3, 471–480, 1995.
Slusser, J. R., Fish, D. J., Strong, E. K., Jones, R. L., Roscoe, H. K., and Sarkissian, A.: Five years of $NO_2$ vertical column measurements at Faraday (65° S): Evidence for the hydrolysis of $BrONO_2$ on Pinatubo aerosols, J. Geophys. Res., 102, D11, 12987–12993, 1997.
Solomon, S., Schmeltekopf, A. L., and Sanders, R. W.: On the interpretation of zenith-sky absorption measurements, J. Geophys. Res., 92, D7, 8311–8319, 1987.
WMO (World Meteorological Organisation), Scientific Assessment of Ozone Depletion: 2006, Global Ozone Research and Monitoring Project – Report No. 50, Geneva, 2007.
Zeng, G. and Pyle, J. A.: Influence of El Nino Southern Oscillation on stratosphere/troposphere exchange and the global tropospheric ozone budget, Geophys. Res. Lett., 32, L01814, doi:10.1029/2004GL021353, 2005.





**Table 1.** Trends in the $NO_2$ vertical column (%/decade) at midsummer sunset between 1990 and 2000 (excluding 1991 and 1992) and between 2000 and 2007, relative to values in 2000. The mean columns at dawn and dusk, calculated using either annual mean intercepts or wavelength shift intercepts, are interpolated to 89°. These trend fits are important for comparison with earlier work on trends in $NO_2$.

| $NO_2$ trends from using annual mean intercepts | | |
|---|---|---|
| | 1990 to 2000 | 2000 to 2007 |
| Dawn | 9±4 | −21±6 |
| Dusk | 11±4 | −22±6 |
| $NO_2$ trends from using wavelength shift intercepts | | |
| | 1990 to 2000 | 2000 to 2007 |
| Dawn | 11±4 | −21±6 |
| Dusk | 13±4 | −22±6 |



ACPD
9, 837–863, 2009



**Table 2.** The trends in the $NO_2$ and $NO_y$ vertical columns (%/decade) at midsummer sunset between 1990 and 2000 (excluding 1991 and 1992) and between 2000 and 2007, relative to values in 2000. The mean $NO_2$ columns at dawn and dusk, using either climatology or observed profiles, are interpolated to 89°, then the $NO_y$ columns are calculated from the $NO_y/NO_2$ ratio for each year.

| $NO_2$ trends using box model results from climatology profiles | | |
|---|---|---|
| | 1990 to 2000 | 2000 to 2007 |
| Dawn | 10±4 | −22±6 |
| Dusk | 12±5 | −22±6 |
| $NO_2$ trends using box model results from observed profiles | | |
| | 1990 to 2000 | 2000 to 2007 |
| Dawn | 9±4 | −21±6 |
| Dusk | 11±5 | −22±6 |
| $NO_y$ trends using box model results from climatology profiles | | |
| | 1990 to 2000 | 2000 to 2007 |
| Dawn | 15±4 | −22±6 |
| Dusk | 17±4 | −22±6 |
| $NO_y$ trends using box model results from observed profiles | | |
| | 1990 to 2000 | 2000 to 2007 |
| Dawn | 13±4 | −22±6 |
| Dusk | 15±5 | −23±5 |



ACPD
9, 837–863, 2009



P. A. Cook and
H. K. Roscoe



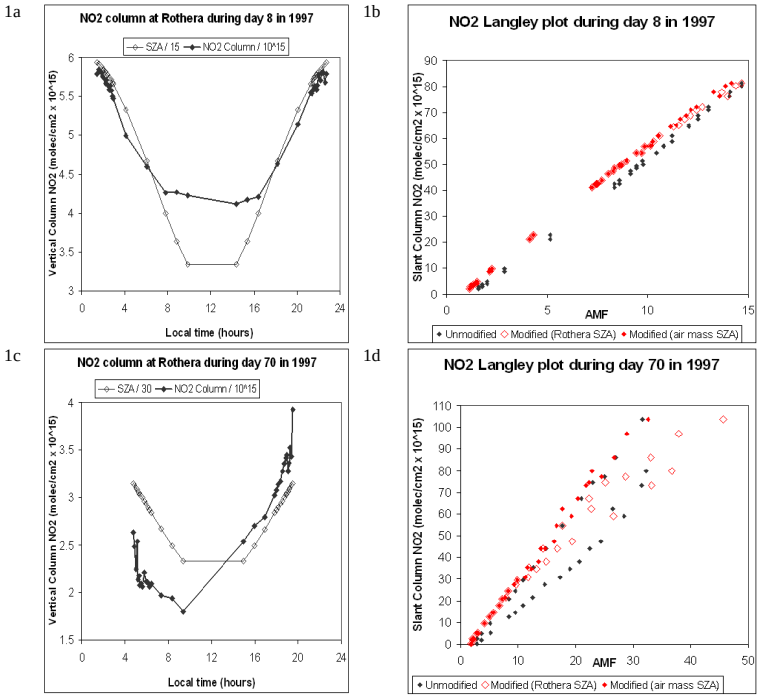


**Fig. 1.** Examples of the daily variation in $NO_2$ with time and SZA, and of the Langley plots produced for the analysis, for days 8 **(a–b)** and 70 **(c–d)** in 1997. Day 8 was in the summer when there was little $N_2O_5$, most of the variation was from the interchange between $NO_2$ and NO, and there is only a small difference between the morning and afternoon columns. However day 70 was in the autumn when most of the variation was from the interchange between $N_2O_5$ and $NO_2$, creating a large difference between the morning and afternoon columns. The Langley plots use unmodified Air Mass Factors (AMFs), AMFs modified by chemical ratios chosen from the Solar Zenith Angles (SZAs) at the spectrometer, and also AMFs modified by chemical ratios chosen from the mean SZAs for the air mass.



ACPD
9, 837–863, 2009



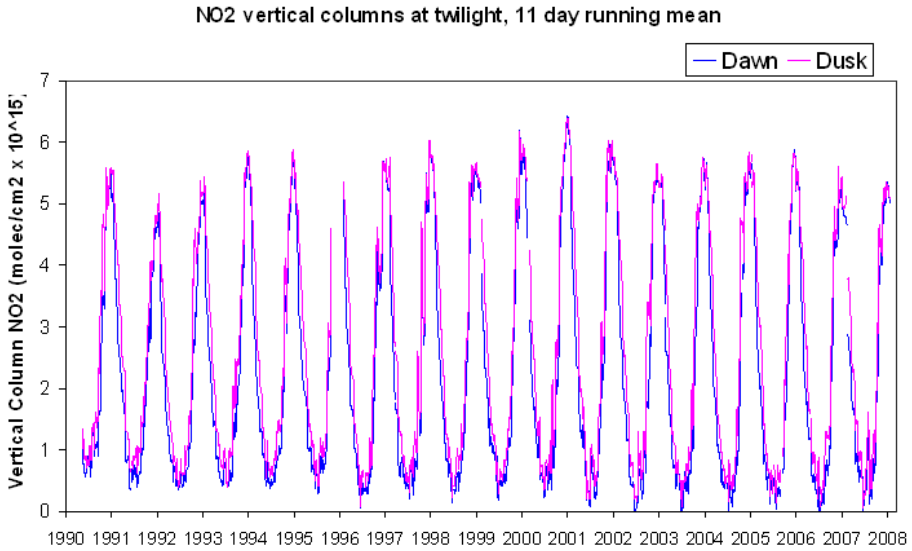


**Fig. 2.** The $NO_2$ vertical columns produced by the analysis at dawn and dusk twilight (87° to 92° SZA) with an 11 day running weighted mean, calculated using annual mean intercepts. The annual cycle of $NO_2$ with midwinter minima and midsummer maxima is clearly seen, and there is more $NO_2$ at dusk than at dawn. The spectrometer was moved from Faraday (65.25° S) to Rothera (67.57° S) in summer 1995 so no measurements were obtained during this period.



ACPD
9, 837–863, 2009



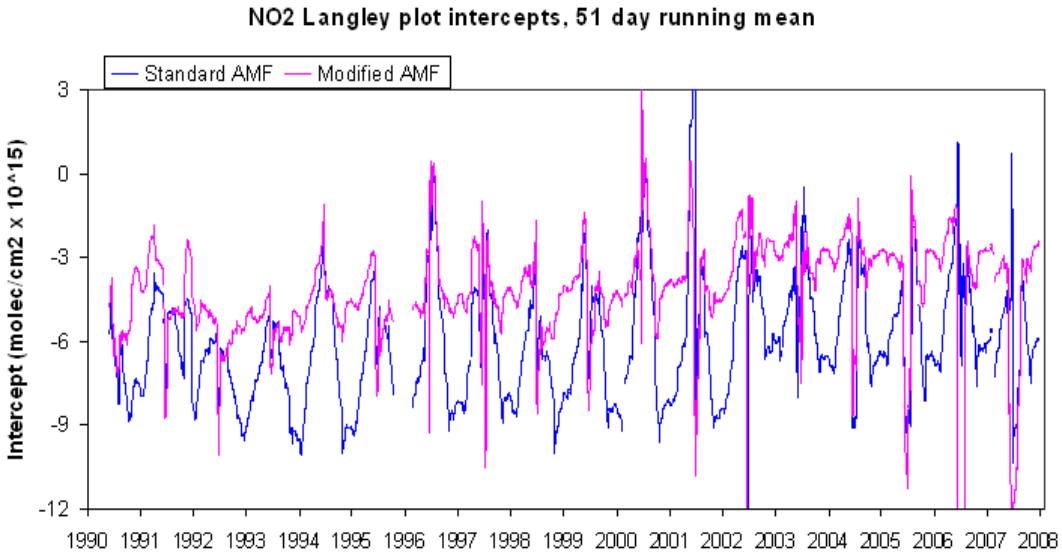


**Fig. 3.** The Langley plot intercepts produced by the analysis using unmodified and modified AMFs, with a 51 day running weighted mean. The modified AMFs produce much smaller intercepts, particularly at midsummer (note that the intercept equals the negative of the amount of $NO_2$ in the reference spectrum, plus any artefact). At midwinter the Langley plots are much poorer and give inaccurate intercept values because little of the $NO_y$ is in the form of $NO_2$, and the range of SZA, and hence AMF, is small.



ACPD
9, 837–863, 2009



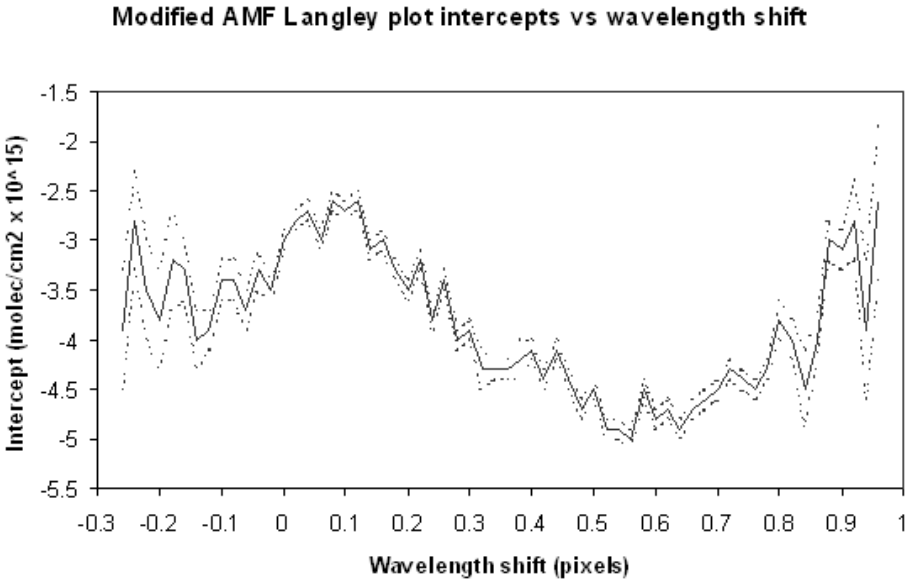


**Fig. 4.** The modified Langley plot intercepts versus the wavelength shift after binning, the solid line is the mean values and the dashed lines the standard deviations. We expect a repeating pattern with minima in the intercepts (small negative values) at shifts of 0 and 1 and maxima (large negative values) at shifts of −0.5 and 0.5. The pattern is actually displaced with a minimum around 0.1 and a maximum around 0.6, presumably due to a bias in the spectral analysis program.



ACPD
9, 837–863, 2009



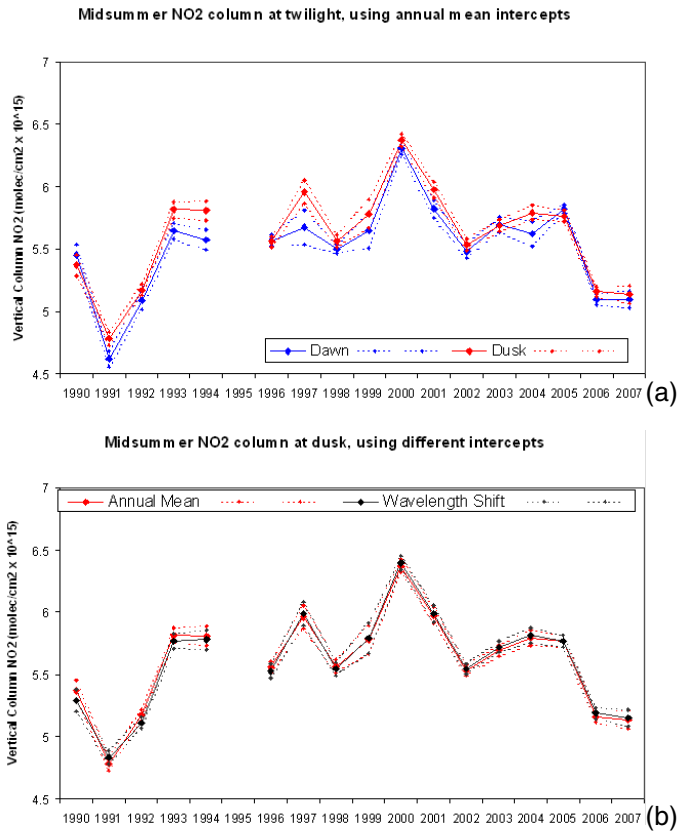


**Fig. 5.** The midsummer $NO_2$ vertical columns at twilight (87° to 92° SZA) for each year, weighted mean and standard deviation for the days 16 to 26 December. **(a)** Dawn and dusk columns calculated using annual weighted mean modified Langley plot intercepts, and **(b)** dusk columns calculated using annual mean intercepts, and daily intercepts estimated from the wavelength shift. There were no midsummer measurements in 1995.



ACPD
9, 837–863, 2009



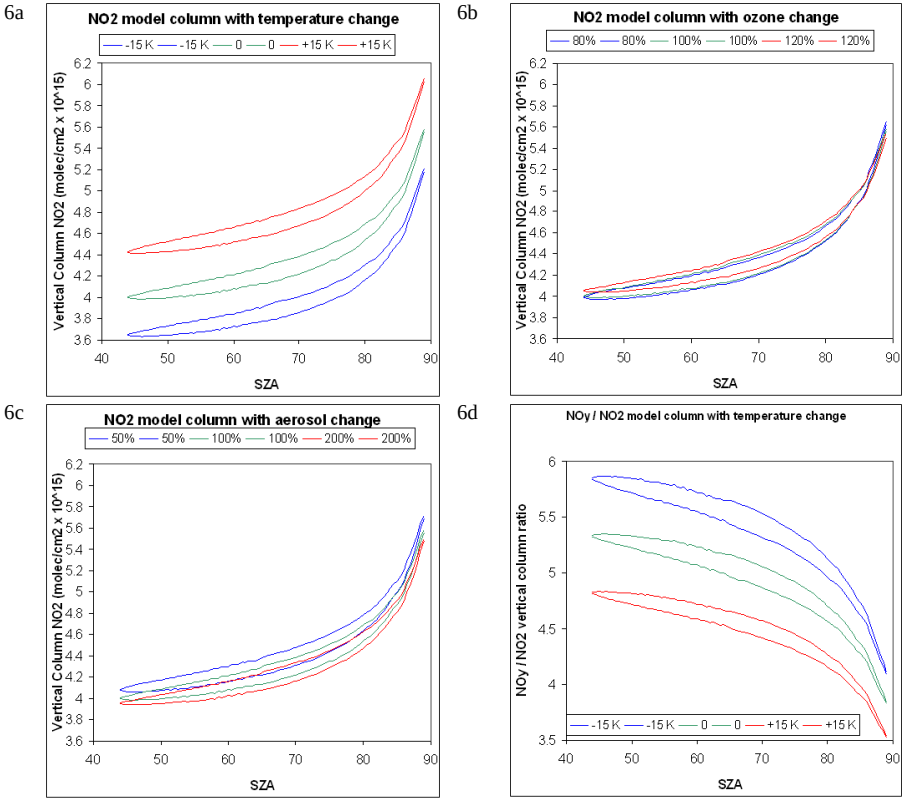


**Fig. 6.** The sensitivity of the box model $NO_2$ vertical column over Rothera in midsummer to temperature, ozone and aerosols, and the sensitivity of the $NO_y/NO_2$ ratio to temperature. Each shows the results from 3 simulations, with the unchanged climatology, and with the input values increased and reduced. **(a)** Stratospheric temperature increased and reduced by 15 K. **(b)** Ozone increased and reduced by 20% at all altitudes. **(c)** Aerosols doubled and halved at all altitudes (changes made to $H_2SO_4$ in the model). **(d)** The $NO_y/NO_2$ ratio in the 3 simulations at different stratospheric temperatures.



ACPD
9, 837–863, 2009



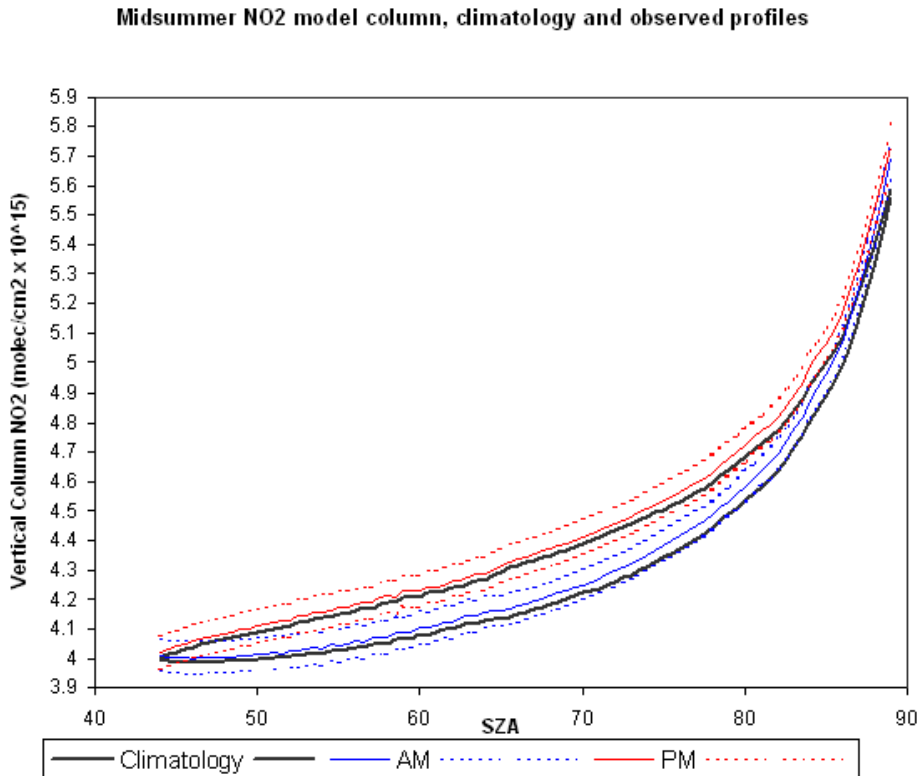


**Fig. 7.** The box model $NO_2$ vertical column over Rothera in midsummer, mean and standard deviation, using the observed temperature and ozone profiles (blue and red lines), and using the climatology (black line).



ACPD
9, 837–863, 2009



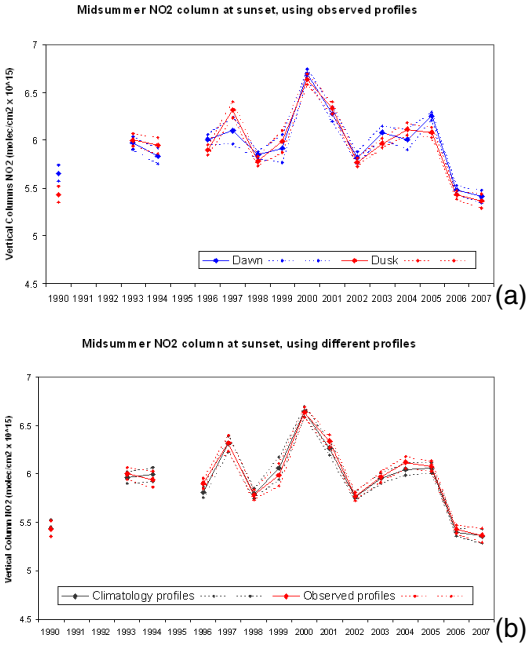


**Fig. 8.** The midsummer mean $NO_2$ vertical columns interpolated to 89° SZA (the maximum SZA at Rothera in midsummer, approximating to sunset). The values at twilight are interpolated according to the weighted mean SZA of the measurements, the diurnal variation of the $NO_2$ column in the box model for each year, and adjusted for the slightly larger $NO_2$ values in the climatology for the lower latitude at Faraday. **(a)** Interpolated dawn and dusk columns from using the observed profiles, and **(b)** interpolated dusk columns using the observed and climatology profiles. Values in 1991 and 1992 were excluded because of the effect in the box model of the greatly increased stratospheric aerosols from the Mt. Pinatubo eruption. In these calculations only the AMFs and $NO_2$ chemical ratios for day 355 were used, and the vertical columns were calculated using midsummer mean modified Langley plot intercepts (1 December to 15 January) rather than annual mean intercepts.



ACPD
9, 837–863, 2009



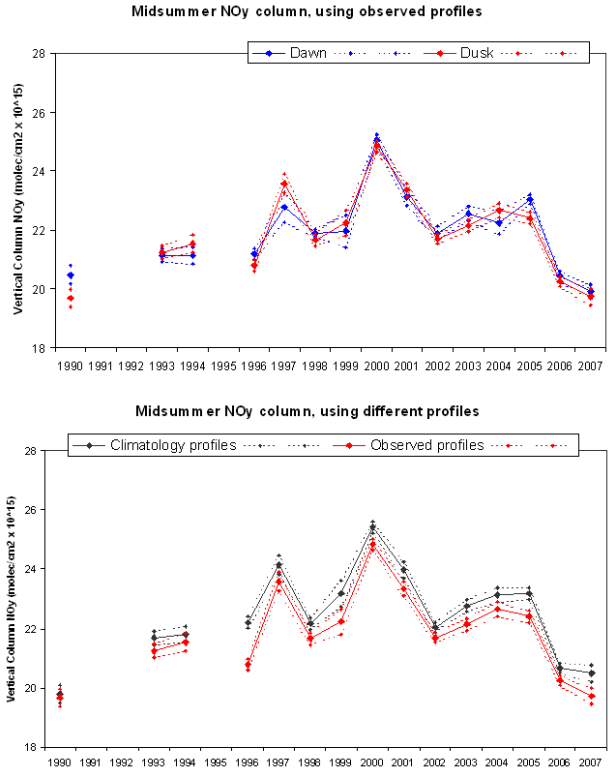


**Fig. 9.** The midsummer $NO_y$ vertical columns, calculated from the $NO_2$ values at 89° SZA in Fig. 8 and the box model $NO_y/NO_2$ ratio at 89° for each year. **(a)** Interpolated dawn and dusk columns using the observed profiles, and **(b)** interpolated dusk columns using the observed and climatology profiles.



ACPD
9, 837–863, 2009